

# **ICON28-POWER2020-16547**

## **COMPUTATIONAL MODELING OF TERRY TURBINE AIRFLOW TESTING TO SUPPORT THE EXPANSION OF OPERATING BAND IN BEYOND DESIGN BASIS CONDITIONS**

### **Lindsay N. Gilkey\***

Structural and Thermal Analysis Dept.  
Sandia National Laboratories  
P.O. Box 5800 M.S. 0748  
Albuquerque, New Mexico 87185  
Email: [Inglke@sandia.gov](mailto:Inglke@sandia.gov)

### **Nathan Andrews**

Accident Consequence Modeling and Analysis Dept.  
Sandia National Laboratories  
P.O. Box 5800 M.S. 0748  
Albuquerque, New Mexico 87185  
Email: [nandrew@sandia.gov](mailto:nandrew@sandia.gov)

### **Kyle Ross**

Sandia National Laboratories (Retired)  
Albuquerque, New Mexico 87185

### **Matthew Solom**

International Nuclear Security Engineering Dept.  
Sandia National Laboratories  
P.O. Box 5800 M.S. 0748  
Albuquerque, New Mexico 87185  
Email: [msolom@sandia.gov](mailto:msolom@sandia.gov)

## **ABSTRACT**

The performance of the Reactor Core Isolation Cooling (RCIC) system under beyond design basis event (BDBE) conditions is not well-characterized. The operating band of the RCIC system is currently specified utilizing conservative assumptions, with restrictive operational guidelines not allowing for an adequate credit of the true capability of the system. For example, it is assumed that battery power is needed for RCIC operation to maintain the reactor pressure vessel (RPV) water level—a loss of battery power is conservatively assumed to result in failure of the RCIC turbopump system in a range of safety and risk assessments. However, the accidents at Fukushima Daiichi Nuclear Power Station (FDNPS) showed that the Unit 2 RCIC did not cease to operate following loss of battery power. In fact, it continued to inject water into the RPV for nearly 3 days following the earthquake. Improved understanding of Terry turbopump operations under BDBE conditions can support enhancement of accident management

procedures and guidelines, promoting more robust severe accident prevention. Therefore, the U.S. Department of Energy (DOE), U.S. nuclear industry, and international stakeholders have funded the Terry Turbine Expanded Operating Band (TTEXOB) program. This program aims to better understand RCIC operations during BDBE conditions through combined experimental and modeling efforts.

As part of the TTEXOB, airflow testing was performed at Texas A&M University (TAMU) of a small-scale ZS-1 and a full-scale GS-2 Terry turbine. This paper presents the corresponding efforts to model operation of the TAMU ZS-1 and GS-2 Terry turbines with Sandia National Laboratories' (SNL) MELCOR code. The current MELCOR modeling approach represents the Terry turbine with a system of equations expressing the conservation of angular momentum. The joint analysis and experimental program identified that a) it is possible for the Terry turbine to develop the same power at different speeds, and b) turbine losses appear to be insensitive to the size of the turbine. As part of this program,

\*Address all correspondence to this author.

*further study of Terry turbine modeling unknowns and uncertainties is planned to support more extensive application of modeling and simulation to the enhancement of plant-specific operational and accident procedures.*

## NOMENCLATURE

$c_{torque}$	Coefficient used to scale the raw torque to match the net torque data.
$c_{windage}$	Loss coefficient scaling the turbine wheel windage.
$M_w$	Moment magnitude scale measure of an earthquake's size.
$m$	Mass flow rate of the air jet through steam nozzles.
$r$	Turbine radius.
$V_{in}$	Velocity of air jet entering turbine buckets.
$V_{out}$	Velocity of air jet leaving turbine buckets.
$\alpha$	Incident angle of air jet relative to incident angle of turbine wheel.
$\omega$	Angular velocity of turbine wheel.

## INTRODUCTION

On March 11, 2011, Japan experienced a magnitude 9 ( $M_w$ ) earthquake, centered at roughly 69 km east of the coast and 32 km deep [1]. The Tohoku earthquake and resulting tsunami caused catastrophic damage to infrastructure and more than 20,000 deaths [1]. The accident progression at Fukushima Daiichi Nuclear Power Station (FDNPS) described in Reference [1] is summarized here. At the site of FDNPS, the earthquake caused a loss of regional power and a scram at 14:46 JST, which resulted in Units 1, 2, and 3 switching to emergency back-up diesel power to maintain reactor pressure vessel (RPV) cooling. At 15:46 JST, the site of FDNPS was inundated by a tsunami wave exceeding 14 meters, leading to station-wide blackout. Units 1, 2, and 3 were left without emergency power and their emergency cooling systems eventually failed.

Unit 2 was equipped with a Reactor Core Isolation Cooling (RCIC) turbopump system, which provided emergency coolant injection to the RPV after the initial loss of onsite power. AC power is assumed to be required for RCIC operation. However, the Unit 2 RCIC did not cease operation after loss of the emergency diesel generators, which occurred roughly 1 hour after the earthquake. In fact, the Unit 2 RCIC provided coolant injection for nearly 3 days [1].

The RCIC system is a steam-driven pumping system which utilizes a G-size frame Terry turbine [2]. The Terry turbine operates by directing steam through a high-pressure steam ring and into a set of expanding nozzles. The expanding nozzles direct the steam tangential to the turbine's buckets, where its flow direction is reversed 180° [2]. Reversing chambers subsequently redirect the steam into the wheel buckets multiple times [2]. A representation of the turbine wheel and the steam flow is in Fig. 1 [3].

The Terry turbine has the following positive attributes: it a) consists of a solid, robust one-piece wheel, b) is insensitive to less than ideal steam conditions, c) quick-starts from cold shutdown, d) has low maintenance requirements, and e) can operate at low pressures [2, 4]. This differs from typical and better characterized turbines, which are generally complex in construction, require a regular maintenance schedule, and operate at high pressures and high efficiencies [4].

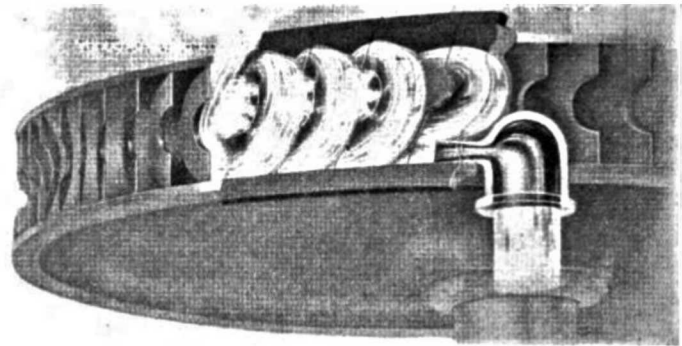


**FIGURE 1: DIAGRAM OF TERRY TURBINE WHEEL, SHOWING STEAM FLOW THROUGH TURBINE BUCKETS, INCLUDING REDIRECTION AS A RESULT OF THE REVERSING CHAMBERS. FIGURE FROM [3].**

Terry turbines have been used for over 100 years [3], however their operation as part of the RCIC turbopump system under beyond design basis event (BDBE) conditions is not well-characterized. The U.S. Department of Energy (DOE), U.S. nuclear industry, and international stakeholders have funded the Terry Turbine Expanded Operating Band (TTEXOB) program to better understand RCIC operations during BDBE conditions through combined experimental and modeling efforts.

During the RCIC operation at FDNPS Unit 2, the RCIC turbopump system ran uncontrolled and successfully maintained RPV levels in degraded operating conditions where it was conservatively anticipated to fail [4]. The Unit 2 RCIC is believed to have run in a mode of operation where the RCIC performance was self-regulated by the RPV level [4]. It is believed that the increased RPV levels led to increased quantities of water in the turbine casing due to water overflowing the RPV and entering the main steam line, which had a negative effect on turbine performance. Turbine pumping power diminished, leading to decreased RPV levels (and water in the RCIC turbine casing) and a following increase in turbine performance. This led to increased RPV levels, and so on, until the time when the Unit 2 RCIC is assumed to have failed after running nearly 3 days in this mode of operation [4]. Capturing and better understanding this dynamic feedback between turbine/pump performance and flow conditions

through modeling and experimentation is one of the main goals of the TTEXOB efforts.

As part of the TTEXOB, air and air-water testing was performed at Texas A&M University (TAMU) of a small-scale ZS-1 and a full-scale GS-2 Terry turbine. This paper presents the corresponding efforts to model operation of air tests of the TAMU GS-2 Terry turbine with MELCOR [5]. MELCOR is a computer code developed at Sandia National Laboratories (SNL) that models severe accident progression in light water reactors [6]. The ZS-1 air test modeling efforts have been previously documented in [7] during 2018.

## TAMU TERRY TURBINE AIRFLOW EXPERIMENTS

Airflow testing was performed at TAMU using a GS-2 and a ZS-1 Terry turbine [8]. A GS-2 Terry turbine has a nominal diameter of 610 mm (24 in) and 10 nozzles [2]. During the TAMU airflow experiments, the upper 5 nozzles were blocked off, which effectively converted the GS-2 to a GS-1 turbine (which only has 5 nozzles on the lower half) [2, 8]. The ZS-1 Terry turbine has a nominal diameter of 457 mm (18 in) and a single nozzle [9]. Additional experiments were performed as part of the TTEXOB, such as two-phase (air and water) testing, however the airflow tests are the only tests modeled for this paper. The experimental configuration of the GS-2 airflow tests is shown in Fig. 2 [8]. The ZS-1 airflow experiments used a very similar experimental configuration, replacing the GS-2 turbine with a ZS-1 turbine.

The experiments characterized turbine performance as a function of airflow and turbine speed. The process used to conduct the experiments and perform data collection was to first use dynamometer loading to bring the turbine to a desired speed at different flow conditions. Once the turbine had reached steady-state at the desired speed, data was collected for the mass flow rate, dynamometer loading, turbine torque, and turbine power. Pressure and temperature information was collected at different locations upstream and downstream of the turbine. The full band of air and air-water tests for the GS-2 turbine were performed for turbine inlet pressure ranging approximately 138 to 483 kPa (20 to 70 psia) [8]. The current modeling of the GS-2 turbine modeled the air tests at  $\sim 345$  kPa (50 psia), which vary in speed from approximately 920 to 3600 RPM. Figure 3 shows the power developed by different airflow tests at different speeds for the range of inlet pressures [8]. One of the notable insights from the TAMU GS-2 airflow testing is the Terry turbine could develop the same power at different speeds. This was also seen in the TAMU ZS-1 airflow testing, which is shown in Fig. 4.

A noteworthy attribute of the airflow experiments that simplified modeling is that the airflow through the steam nozzle was choked. Choked flow is a limiting condition where further lowering pressure downstream of the nozzle terminus does not affect the mass flow rate [11]. This allowed for modeling simplifications in MELCOR to be performed which will be discussed in the

following section.

## MODELING APPROACH AND DESCRIPTION

MELCOR modeling was performed for the GS-2 airflow tests corresponding to nozzle inlet pressure at approximately 345 kPa. MELCOR modeling has been performed for the ZS-1 airflow tests, however they are not the focus of this paper and are documented elsewhere [7]. A visual representation of the MELCOR model nodalization is shown in Fig. 5. The piping and flow paths shown in Fig. 2 were simplified so only piping directly upstream and downstream of the turbine inlet and exhaust were represented. In future iterations of this model, the full flowpath geometry will be represented and will include modifications for modeling the two-phase air-water tests performed at TAMU. The airflow tests were modeled first as they are simpler to implement and are a foundation for more advanced RCIC modeling, such as two-phase modeling and the FDNPS Unit 2 modeling (which may operate under two-phase steam-water conditions [1, 4]).

The approach taken during the MELCOR modeling was for a given experiment, the air tank pressure and temperature were set in the MELCOR model to match the pressure/temperature sensor data recorded upstream of the turbine inlet. The valve opening fraction (shown in Fig. 5) was then adjusted to restrict the flow path until the desired mass flow rate developed. For the  $\sim 345$  kPa air tests for the GS-2 turbine, the air mass flow rate was approximately 0.69-0.72 kg/s. Trial and error determined the valve opening fraction that developed the correct mass flow rate and turbine inlet pressure/temperature recorded in the experiment.

In MELCOR, the nozzle region is characterized by a specification of the nozzle length and exit geometry. As MELCOR is a control volume code, it cannot be used to determine supersonic quantities, i.e., the supersonic velocity of the air entering or exiting the Terry turbine buckets. These quantities were determined through prior computational fluid dynamics (CFD) analysis of a Terry turbine at varying pressures [7] and were tabulated in the MELCOR model. For a given nozzle inlet pressure, the MELCOR model used the table values to interpolate values for the supersonic air velocity entering and exiting the turbine buckets, which were then used in the representation of the Terry turbine discussed below. The flow of air then exits the turbine casing to the environment, which is a flowpath geometry simplification enabled by the choked flow observed in the experiment.

The MELCOR modeling representation of the Terry turbine utilizes control functions to express a system of equations for the conservation of angular momentum and to calculate turbine torque. If modeling a Terry turbopump system (with a pump), the turbine torque control function is used as an input to the RCIC pump, which is modeled by the flow path package's homologous pump model. The TAMU airflow experiments however did not include a pump; therefore it was not included in the modeling.

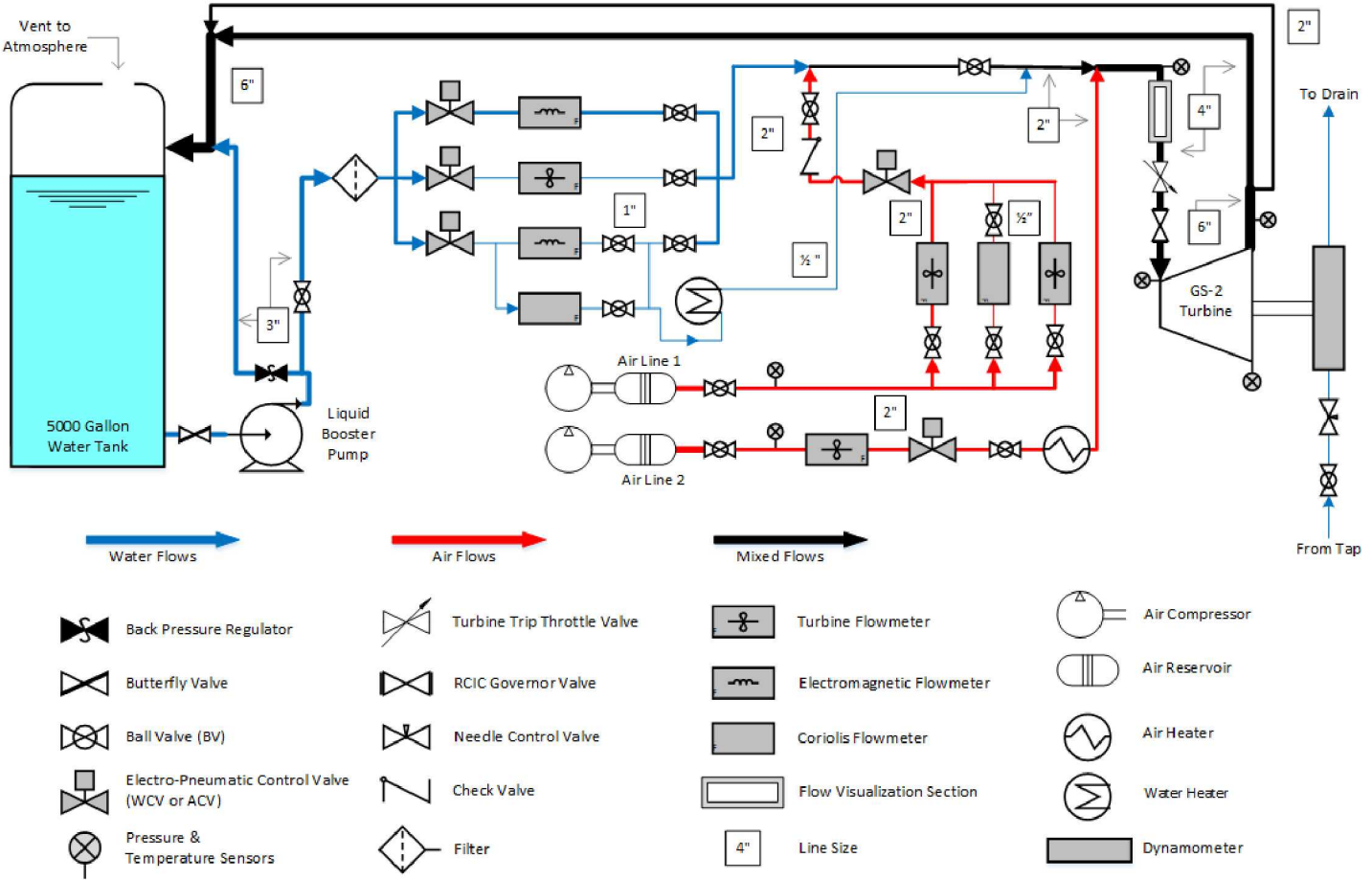


**FIGURE 2:** EXPERIMENTAL CONFIGURATION OF GS-2 AIR-BASED TESTS. FIGURE FROM [8].

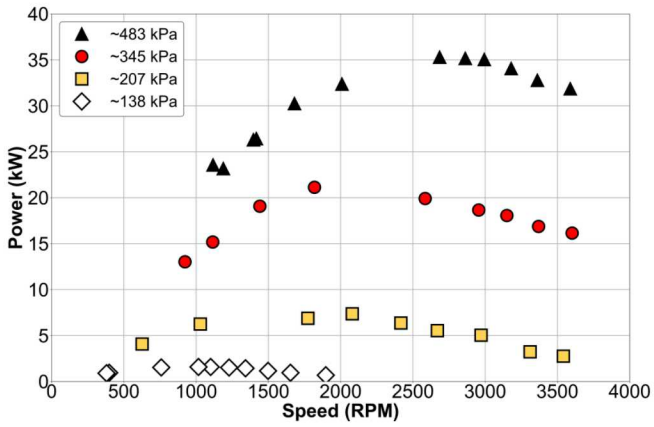


**FIGURE 3:** EXPERIMENTALLY DETERMINED GS-2 POWER VS. SPEED OF AIR-BASED TESTS (COLORED BY APPROXIMATE INLET PRESSURE) [8].

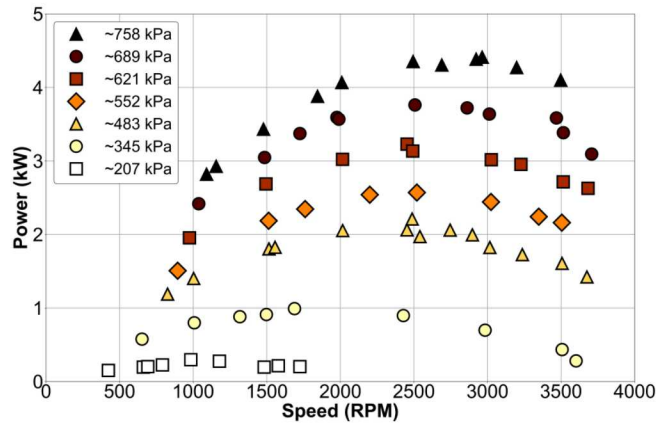


**FIGURE 4:** EXPERIMENTALLY DETERMINED ZS-1 POWER VS. SPEED OF AIR-BASED TESTS (COLORED BY APPROXIMATE INLET PRESSURE). FIGURE ADAPTED FROM [10].

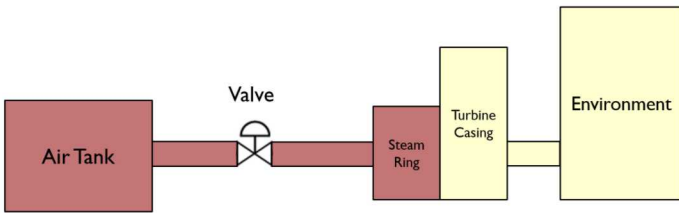


**FIGURE 5:** MELCOR MODELING NODALIZATION OF THE TAMU AIRFLOW EXPERIMENTS.

The equation for the raw turbine torque is:

$$\text{torque}_{\text{raw}} = r \times \dot{m} \times c_{\text{torque}} \times [(V_{\text{in}} - V_{\text{out}}) \cos \alpha - 2r\omega] \quad (1)$$

where  $r$  is turbine radius,  $\dot{m}$  is the mass flow rate of the jet through the steam nozzles,  $c_{\text{torque}}$  is a coefficient used to scale the raw torque to match the net torque data,  $V_{\text{in}}$  and  $V_{\text{out}}$  are the velocities of the jet entering or leaving the turbine buckets,  $\alpha$  is the incident angle of the jet relative to the incident angle of the turbine wheel, and  $\omega$  is the angular velocity of the turbine wheel.

Wheel windage resists the wheel motion and is represented with the following form:

$$\text{windage} = c_{\text{windage}} \times \omega^2 \quad (2)$$

where  $c_{\text{windage}}$  is a loss coefficient scaling the total windage losses. The net turbine torque is therefore:

$$\text{torque}_{\text{net}} = \text{torque}_{\text{raw}} - \text{windage} \quad (3)$$

In Eqn. 1 and 2, coefficients  $c_{\text{torque}}$  and  $c_{\text{windage}}$  are determined through calibration such that the model net turbine power and torque match the experimental value at a given turbine speed, nozzle condition, and dynamometer peak resistive torque. The modeling procedure is to bring the turbine slowly up from zero speed to a steady-state condition either at the experimentally recorded speed or the peak model speed if this value is lower than the experimentally determined speed. At steady-state, net torque and turbine power are recorded and can be compared to the experimental values.

The significant geometry differences between the ZS-1 and GS-2 Terry turbine are the following:

- The ZS-1 model has 1 nozzle and turbine radius of 457 mm.
- The GS-2 model has 5 nozzles and turbine radius of 610 mm.

The differences in turbine radius was represented in the MELCOR modeling by the assumed size of the turbine casing and the turbine radius ( $r$ ) in Eqn. 1.

## MELCOR MODELING RESULTS

The GS-2 airflow tests performed at nozzle inlet pressure  $\sim 345$  kPa were selected for modeling. The goal of the modeling was to predict the power vs. speed observed in the airflow experiments at different flow conditions. Responses of torque, power, and speed were collected for comparison to experimental data. Additional discussion of these results can be found in [5].

The coefficients  $c_{\text{windage}}$  and  $c_{\text{torque}}$  in Eqn. 1 and 2 were determined through calibration. The current calibration approach utilized was to use values of  $c_{\text{windage}}$  and  $c_{\text{torque}}$  previously identified for the smaller ZS-1 turbine during air test modeling as an initial calibration point. A single experiment was then selected to use for calibration data. The 1818 RPM test (Fig. 3) was identified as the “peak efficiency” case for the  $\sim 345$  kPa inlet pressure experiments and was selected for calibration. Calibration was performed using a least-squares algorithm to minimize the residuals of experimental and model speed and net turbine power. Once the calibration yielded a calibrated value of  $c_{\text{windage}}$  and  $c_{\text{torque}}$ , the values were applied to the remaining airflow tests at  $\sim 345$  kPa. This specific approach was chosen as it was previously used for the ZS-1.

An alternative strategy that will be employed in the future is to split the experimental data into calibration and validation sets, determine calibrated coefficients that best fit the calibration set data, and then apply the calibrated coefficients to the validation set models. It would also be useful to weight higher speed tests more in the calibration of the  $c_{\text{windage}}$  term as the windage losses are relatively insignificant at lower turbine speeds.

Figure 6 shows the speed time-history response of the GS-2 airflow  $\sim 345$  kPa case at 1818 RPM, where the turbine starts at zero speed and quickly reaches the experimentally observed peak speed. Figure 7 shows the power time-history model response of the GS-2 airflow  $\sim 345$  kPa case at 1818 RPM. In this figure, windage is represented as a negative quantity as it acts as a loss. In this specific case, windage losses are not significant. However, at a higher speed test at 3601 RPM (Fig. 8) windage losses do significantly reduce the net turbine power. This is anticipated as windage losses scale by turbine speed squared.

The coefficients  $c_{\text{windage}}$  and  $c_{\text{torque}}$  determined by calibration for the ZS-1 and GS-2 turbines are listed in Tab. 1. The turbines are different sizes and have different associated flow conditions, however their coefficients values are similar. The GS-2 air tests at  $\sim 345$  kPa were modeled using the ZS-1 determined and GS-2 determined coefficients. Figure 9 shows plots of power vs. speed for the GS-2 air test experiments, the GS-2 air test models using the ZS-1 air test determined calibrated coefficients, and the GS-2 air test models using the GS-2 air test determined calibrated coefficients. Figures 10 and 11 show the MELCOR power or speed vs. the measured power or speed. The power and speed values are also recorded in Tab. 2.

The GS-2 coefficient results in Fig. 9 and Tab. 2 follow the power vs. speed trends observed in the experiment. The coeffi-

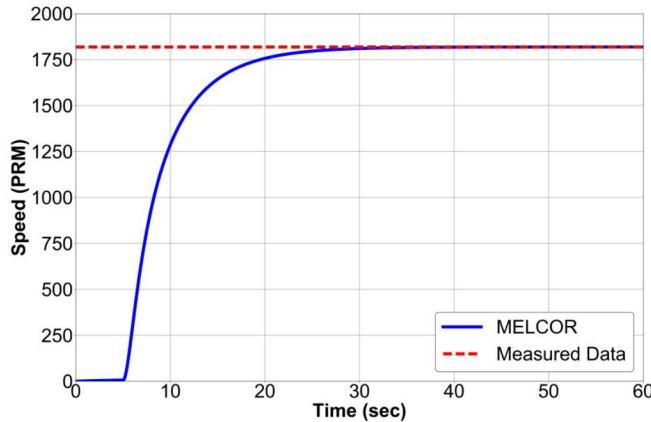


**FIGURE 6:** MELCOR MODELED SPEED TIME-HISTORY RESPONSE OF GS-2 AIRFLOW EXPERIMENT AT  $\sim 345$  kPa AND 1818 RPM.

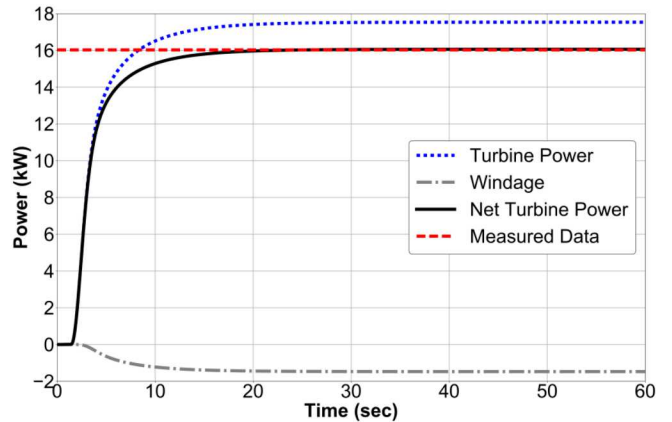


**FIGURE 8:** MELCOR MODELED POWER TIME-HISTORY RESPONSE OF GS-2 AIRFLOW EXPERIMENT AT  $\sim 345$  kPa AND 3601 RPM.

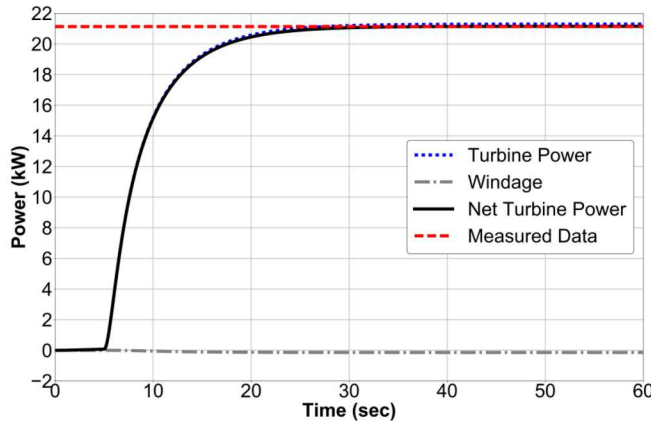


**FIGURE 7:** MELCOR MODELED POWER TIME-HISTORY RESPONSE OF GS-2 AIRFLOW EXPERIMENT AT  $\sim 345$  kPa AND 1818 RPM.

**TABLE 1:** ZS-1 AND GS-2 DETERMINED CALIBRATED COEFFICIENTS.

Turbine	$c_{windage}$	$c_{torque}$
ZS-1	$4.50 \times 10^{-7}$	2.32
GS-2	$3.07 \times 10^{-7}$	2.53

ients were calibrated to match the  $\sim 345$  kPa, 1818 RPM case experimental power and speed, so this point is anticipated to match

the experiment. The GS-2 coefficient results overpredict the power at observed speeds higher than 1818 RPM, however the model result at 3601 RPM closely matches the experimental data, as seen in Fig. 10.

The ZS-1 coefficient results match the power vs. speed trends observed in the experiment, however the model results underpredict the power vs. speed curve (Fig. 10). This may be attributed to the increased  $c_{windage}$  and decreased  $c_{torque}$  coefficients when compared to the GS-2 determined values. Increased  $c_{windage}$  results in increased losses, especially at higher speeds as the windage loss scales with turbine speed squared, and decreased  $c_{torque}$  results in a loss of raw turbine torque for a given set of flow conditions, so it is anticipated that the power vs. speed predictions using the ZS-1 coefficients would be less than the predictions using the GS-2 determined coefficients. As an example, this can be seen in Fig. 12, which compares the power time-histories of the GS-2 model at the 3601 RPM (experimental speed) case using the ZS-1 and GS-2 determined coefficients. In this plot, even though the ZS-1 coefficient case reaches a lower peak speed than the GS-2 coefficient case, its windage losses are greater. The ZS-1 coefficient model results also did not achieve the peak speed recorded in the experiment, which can be observed in Fig. 11. This is most apparent at turbine speeds lower than approximately 2500 RPM. The ZS-1 coefficient model however performs nearly as well as the GS-2 coefficient model at the higher speed flow conditions for the GS-2 air tests. Both sets of determined coefficients also captured the behavior of the same turbine power being developed at different turbine speeds.

The results shown in Fig. 9 are noteworthy as the similar results obtained using the different sets of coefficients may indicate that the coefficients are not scaled with turbine size (assumed prior to this analysis). For RCIC turbine modeling, this would

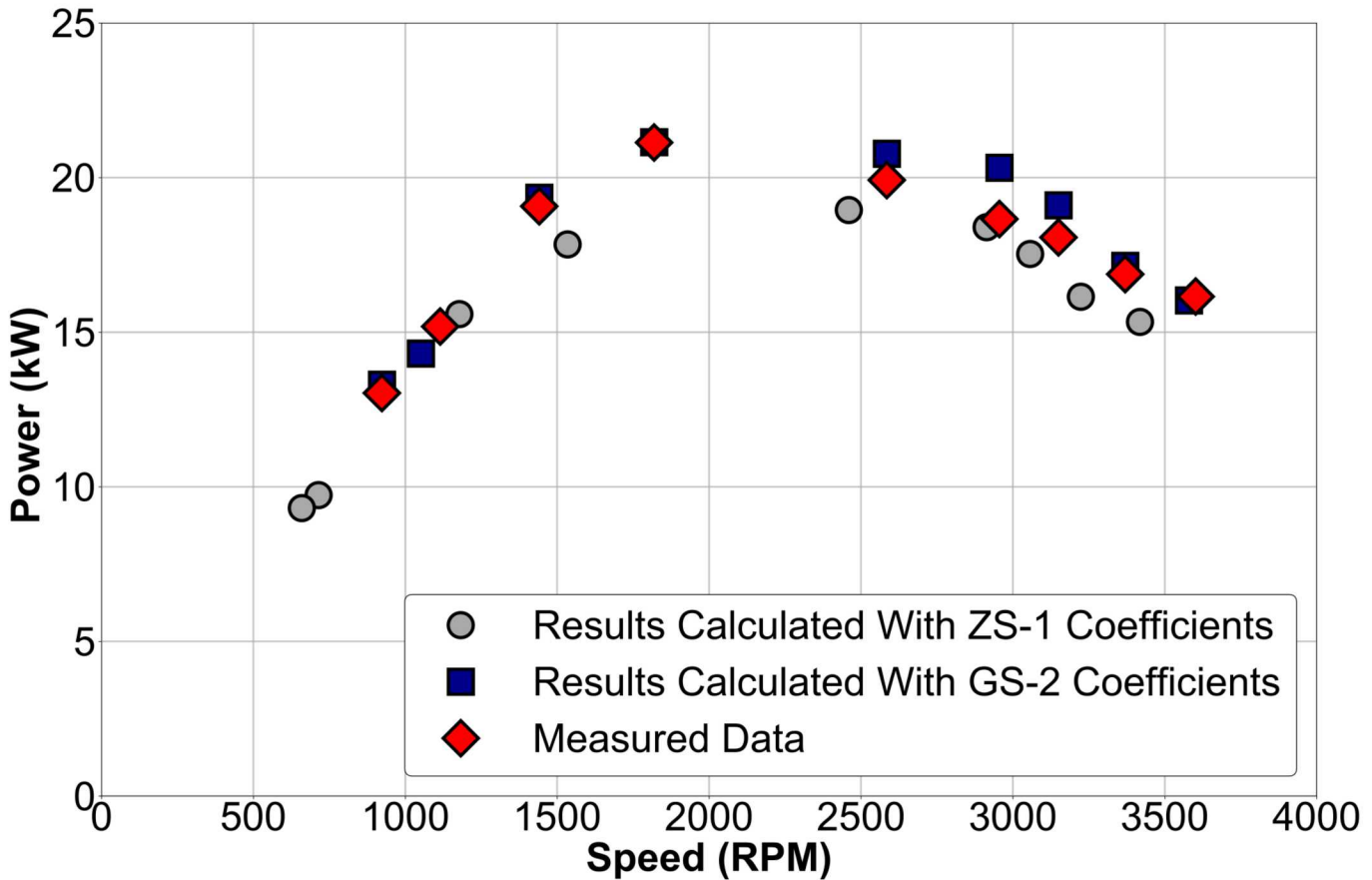


**FIGURE 9: POWER VS. SPEED OF THE GS-2 AIR TESTS PERFORMED AT TURBINE INLET PRESSURE  $\sim 345$  kPa EXPERIMENTAL VALUES COMPARED TO THE MODELED RESPONSES USING THE ZS-1 AND GS-2 CALIBRATED COEFFICIENTS FOR WINDAGE LOSS AND RAW TORQUE (TAB. 1).**

indicate that the coefficients associated with raw torque and losses are relatively insensitive to turbine size and that the effects of turbine size have been captured in the RCIC governing equations in MELCOR modeling. The coefficients are anticipated to scale based on fluid density. The relative coefficient insensitivity to size and the anticipated scaling due to fluid density should be further investigated by additional modeling of experiments. Additional air tests for the ZS-1 and GS-2 TAMU Terry turbines can be modeled to verify if the apparent coefficient insensitivity due to turbine size is observed at a wider range of turbine flow conditions. Steam and air-water tests will be used to determine the scaling of the coefficients due to fluid density.

#### OBSERVATIONS AND RECOMMENDATIONS FOR FUTURE STUDY

For the GS-2 airflow MELCOR modeling, the effects of the turbine size scaling in the RCIC governing equations and the determination of the turbine coefficients have been identified as important Terry turbine modeling unknowns that warrant additional investigation through experimentation and modeling. Effective modeling approaches need to address and resolve these modeling unknowns (as well as additional unknowns that have yet to be identified) to accurately predict the Terry turbine response during different flow conditions.

The turbine size scaling was assumed prior to the current modeling of the GS-2 Terry turbine to be captured by scaling of the coefficients  $c_{torque}$  and  $c_{windage}$  and changing the radius ( $r$ ) in Eqn. 1 and 2. The current model results showed that applying the coefficients determined using the smaller radius ZS-1 turbine

**TABLE 2:** EXPERIMENTAL, ZS-1, AND GS-2 COEFFICIENTS RESULTS COMPARED FOR THE INLET PRESSURE  $\sim 345$  kPa AIR TESTS. DATA SHOWN IN FIG. 9, 10, and 11.

Experiment		Results Calculated With ZS-1 Coefficients		Results Calculated With GS-2 Coefficients	
Speed (RPM)	Power (kW)	Speed (RPM)	Power (kW)	Speed (RPM)	Power (kW)
3601	16.2	3418	15.3	3579	16.0
3369	16.9	3224	16.1	3369	17.2
3150	18.1	3056	17.5	3150	19.1
2955	18.7	2913	18.4	2955	20.3
2585	19.9	2460	19.0	2585	20.8
1818	21.1	1534	17.8	1818	21.1
1441	19.1	1178	15.6	1441	19.4
1115	15.2	715	9.7	1051	14.3
922	13.0	659	9.3	922	13.3

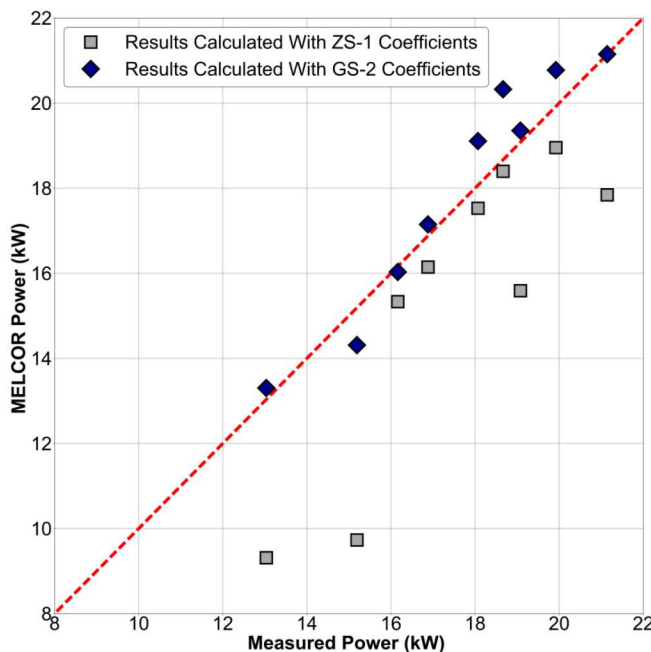


**FIGURE 10:** MELCOR POWER VS. MEASURED POWER OF THE GS-2 AIR TESTS PERFORMED AT TURBINE INLET PRESSURE  $\sim 345$  kPa USING THE ZS-1 AND GS-2 CALIBRATED COEFFICIENTS FOR WINDAGE LOSS AND RAW TORQUE (TAB. 1).

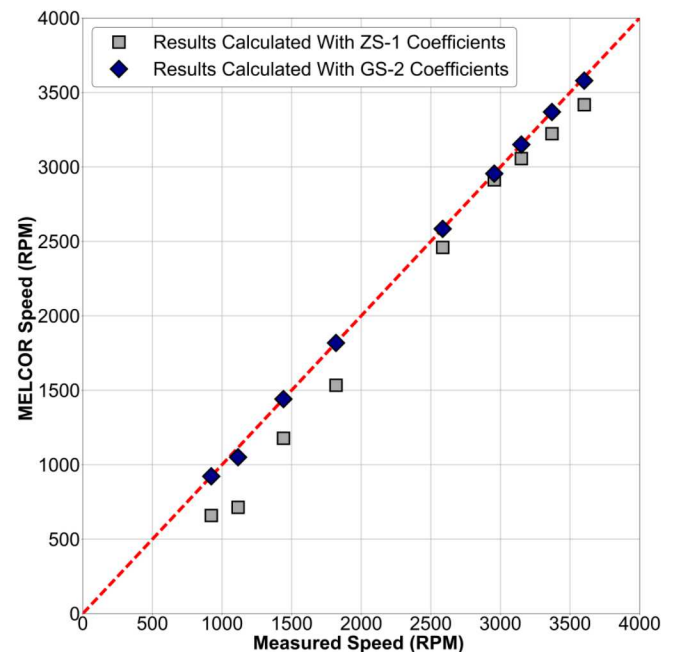


**FIGURE 11:** MELCOR SPEED VS. MEASURED SPEED OF THE GS-2 AIR TESTS PERFORMED AT TURBINE INLET PRESSURE  $\sim 345$  kPa USING THE ZS-1 AND GS-2 CALIBRATED COEFFICIENTS FOR WINDAGE LOSS AND RAW TORQUE (TAB. 1).

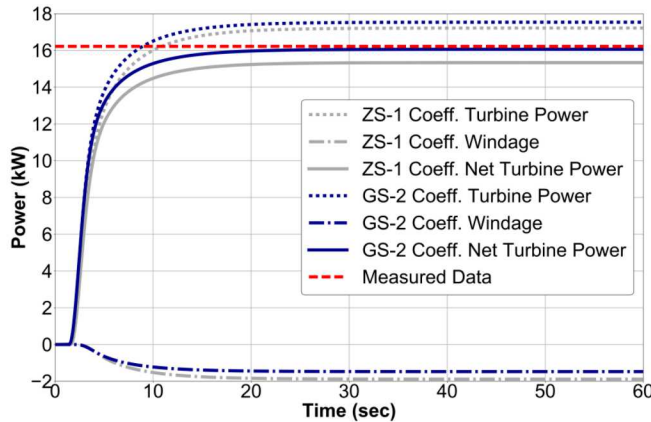


**FIGURE 12: MELCOR MODELED POWER TIME-HISTORY RESPONSE OF GS-2 AIRFLOW EXPERIMENT AT  $\sim 345$  kPa AND 3601 RPM, COMPARING THE GS-2 MODEL USING THE ZS-1 AND GS-2 COEFFICIENTS (TAB. 1).**

to the larger GS-2 turbine produced model predictions that captured the power vs. speed trends observed in the experiment. At higher speeds, the model predictions of the ZS-1 determined coefficients applied to the GS-2 turbine performed nearly as well as the GS-2 determined coefficients at matching the experimental power vs. speed data. These coefficients appear to be relatively insensitive to turbine size from the current modeling, however additional modeling is required to validate this conclusion. It is possible that the effects of size scaling between the turbines was adequately captured by the Terry turbine model governing equations and does not need to be reflected in coefficient scaling. The current results imply that size scaling effects were folded into the Terry turbine equations and representation, however this was for a relatively narrow range of flow conditions. Additional airflow data was collected for the ZS-1 and GS-2 Terry turbines, which can be modeled to address the modeling unknown of the scaling according to turbine size.

Additionally, the turbine coefficients are identified as an important modeling unknown for predicting Terry turbine performance. Windage losses are scaled by the turbine speed squared, therefore the value of  $c_{windage}$  is significant at high speeds. The raw torque is scaled by the  $c_{torque}$ , so correct determination of this value is also important for accurate predictions. However, the experimental data only reported values of net torque, which is shown in Eqn. 3 to be the sum of the raw torque and windage losses. Calibration of  $c_{windage}$  and  $c_{torque}$  to the data may yield multiple suitable coefficient pairs. This modeling unknown should be addressed by modeling of the additional GS-2 airflow tests. The coefficients can be determined by calibration to minimize the residuals for 1) each individual experiment and 2) all the experiments. This will yield multiple coefficient pairs, which can then be used to bet-

ter assess the coefficient pairs and have greater confidence in their anticipated ranges and variance. Bayesian calibration would yield additional information, i.e., calibrated coefficients and their distributions, however additional analysis is needed to determine if this problem is suitable for Bayesian calibration as the Bayesian calibration process is very time-consuming. It would also be valuable to perform the aforementioned calibration exercise with the ZS-1 model and data. This would help address the modeling unknown of the coefficient scaling according to turbine size. As mentioned previously, the coefficients are assumed to scale according to fluid density. This was not investigated with the current GS-2 modeling. Steam or air-water test data can be used to address this modeling unknown.

The GS-2 airflow modeling captured the same trends observed from the TAMU Terry turbine airflow testing, most notably the same power being developed at different turbine speeds for the same approximate inlet pressure. This was also seen during the previous ZS-1 TAMU airflow testing and modeling. Correctly capturing this phenomenon in modeling is important for predictions of RCIC operations and gaining better understanding of how the system responds during BDBEs. The current modeling was successful at capturing results consistent with experimentally observed behavior, but additional modeling will help gain better understanding of this phenomenon, especially at high turbine speeds where windage losses become more significant.

It is challenging to apply RCIC modeling to the actual plant modeling as there are other losses in the system that are either unknown or difficult to quantify with the limited data available. By modeling and characterizing the Terry turbine performance of the TAMU ZS-1 and GS-2 turbines, we gain valuable insight into how the Terry turbine operates and how it should be characterized and applied as part of the integral plant response. Future work as part of the TTEXOB includes applying detailed models of the RCIC operations as part of the integral plant response of the FDNPS Unit 2 modeling and capturing the dynamic and self-regulating response of the RCIC turbopump.

## CONCLUSIONS

The current approach of modeling the GS-2 Terry turbine was effective at predicting the developed turbine power for a given turbine speed and flow condition, however modeling unknowns need to be addressed to support more extensive application of modeling and simulation to the enhancement of plant-specific operational and accident procedures. The modeling of the ZS-1 and GS-2 turbines is being performed parallel to MELCOR efforts at SNL to model the response of FDNPS Unit 2, with emphasis on the RCIC system response. Improving the ZS-1 and GS-2 TAMU Terry turbine models will inform modeling decisions made pertaining to the implementation of the Unit 2 RCIC turbopump model and overall support informed enhancement of severe accident management procedures and guidelines.

## ACKNOWLEDGMENT

Sandia National Laboratories is a multimission laboratory managed and operated by National Technology and Engineering Solutions of Sandia, LLC, a wholly owned subsidiary of Honeywell International, Inc., for the U.S. Department of Energy's National Nuclear Security Administration under contract DE-NA0003525. SAND2020-XXXX

## REFERENCES

- [1] Gauntt, R., Kalinich, D., Cardoni, J., Phillips, J., Goldmann, A., Pickering, S., Francis, M., Robb, K., Ott, L., Wang, D., Smith, C., St.Germain, S., Schwieder, D., and Phelan, C., July 2012. *Fukushima Daiichi Accident Study (Status as of April 2012)*. Sandia National Laboratories, Albuquerque, NM, U.S.A. SAND2012-6173.
- [2] Kelso, J., et al., 2012. *Terry Turbine Maintenance Guide, RCIC Application: Replaces TR-105874 and TR-016909-R1*. Electric Power Research Institute, Palo Alto, CA, U.S.A. EPRI Technical Report Number 1007460.
- [3] Unknown Author, 1918. “The Terry turbine-driven fans”. *Journal of the American Society of Naval Engineers*, **30**(1), pp. 598–599.
- [4] Ross, K., Cardoni, J., Wilson, C., Morrow, C., Osborn, D., and Gauntt, R., December 2015. *Modeling of the Reactor Core Isolation Cooling Response to Beyond Design Basis Operations – Phase 1*. Sandia National Laboratories, Albuquerque, NM, U.S.A. SAND2015-10662.
- [5] Gilkey, L., Solom, M., and Andrews, N., October 2019. *Terry Turbopump Expanded Operating Band Modeling and Full-Scale Test Development Efforts in Fiscal Year 2019 - Progress Report*. Sandia National Laboratories, Albuquerque, NM, U.S.A. SAND2019-13423.
- [6] Humphries, L., Beeney, B., Gelbard, F., Louie, D., and Phillips, J., October 2019. *MELCOR Computer Code Manuals, Vol. 1: Primer and Users' Guide, Version 2.2.14959*. Sandia National Laboratories, Albuquerque, NM, U.S.A. SAND2019-12536 O.
- [7] Cardoni, J., Ross, K., and Osborn, D., September 2018. *Terry Turbopump Analytical Modeling Efforts in Fiscal Year 2018 – Progress Report*. Sandia National Laboratories, Albuquerque, NM, U.S.A. SAND2018-10133.
- [8] Solom, M., Osborn, D., and Andrews, N., 2019. *OUO: RCIC Experimental Review Report*. Sandia National Laboratories, Albuquerque, NM, U.S.A.
- [9] THE TERRY STEAM TURBINE CO., 1959. *Terry Instruction Manual Type Z-1 and ZS-1*. Hartford, CT, U.S.A.
- [10] Patil, A., Wang, Y., Solom, M., Alfandi, A., Sundar, S., Vierow Kirkland, K., and Morrison, G., 2020. “Two-phase operation of a Terry steam turbine using air and water mixtures as working fluids”. *Applied Thermal Engineering*, **165**, p. 114567.
- [11] Zucker, R., and Biblarz, O., 2002. *Fundamentals of Gas Dynamics*. Hoboken, NJ, U.S.A.